

# Taylor expansion MUSIC method for joint DOD and DOA estimation in a bistatic MIMO array\*

Wen-tao SHI<sup>†‡1,2</sup>, Qun-fei ZHANG<sup>1</sup>, Cheng-bing HE<sup>1</sup>, Jing HAN<sup>1</sup>

<sup>1</sup>*School of Marine Science and Technology, Northwestern Polytechnical University, Xi'an 710072, China*

<sup>2</sup>*Science and Technology on Electronic Information Control Laboratory, Chengdu 610041, China*

<sup>†</sup>E-mail: swt@nwpu.edu.cn

Received Oct. 8, 2017; Revision accepted Sept. 28, 2018; Crosschecked June 11, 2019

**Abstract:** We propose a Taylor expansion multiple signal classification (TE MUSIC) method for joint direction of departure (DOD) and direction of arrival (DOA) estimation in a bistatic multiple-input multiple-output (MIMO) array. First, using a Taylor expansion of the steering vector, a two-dimensional (2D) search in the conventional MUSIC method for MIMO arrays is reduced to a two-step one-dimensional (1D) search in the proposed TE MUSIC method. Second, DOAs of the targets can be achieved via Lagrange multiplier by a 1D search. Finally, substituting the DOA estimates into the 2D MUSIC spectrum function, DODs of the targets are obtained by another 1D search. Thus, the DOD and DOA estimates can be automatically paired. The performance of the proposed method is better than that of the MIMO ESPRIT method, and is similar to that of the 2D MUSIC method. Furthermore, due to the 1D search, the TE MUSIC method avoids the high computational complexity of the 2D MUSIC method. Simulation results are presented to show the effectiveness of the proposed method.

**Key words:** Bistatic multiple-input multiple-output array; Direction of departure; Direction of arrival; Multiple signal classification; Taylor expansion; Computational complexity

<https://doi.org/10.1631/FITEE.1700657>

**CLC number:** TP391.4

## 1 Introduction

Multiple-input multiple-output (MIMO) array has been a subject of considerable research and development for its potential advantages over conventional phased-array systems (Fishler et al., 2004a; Bekkerman and Tabrikian, 2006; Zhang and Zhu, 2013; Guo et al., 2015; Yeo et al., 2017). The MIMO array uses multiple antennas to emit independent waveforms, and exploits multiple antennas in receiving reflected signals. According to the configuration,

MIMO arrays can be classified into two categories. The first category is the statistical MIMO array (Fishler et al., 2004b, 2006; Haimovich et al., 2008; Ai et al., 2015; Sharify and Nayebi, 2017), whose transmit antennas or both transmit and receive antennas are located far from each other to achieve a spatial diversity gain. This MIMO array framework can overcome performance degradation caused by target scintillations. The other category is the monostatic or bistatic MIMO array (Robey et al., 2004; Li and Stoica, 2007; Xu et al., 2008; Zheng and Chen, 2015; Zheng et al., 2016; Cao et al., 2017). In this category, transmit and receive antennas are closely spaced, and can provide many high-resolution angle estimations, thus achieving flexible spatial transmit beam-pattern design and significantly improving parameter identifiability. In this study, we focus on the second category.

<sup>‡</sup> Corresponding author

\* Project supported by the National Natural Science Foundation of China (Nos. 61501374 and 61531015), the Fundamental Research Funds for the Central Universities, China (No. 3102015ZY084), and the Project of Science and Technology on Electronic Information Control Laboratory, China

 ORCID: Wen-tao SHI, <http://orcid.org/0000-0002-0847-9701>

© Zhejiang University and Springer-Verlag GmbH Germany, part of Springer Nature 2019

Researchers have great interest in the bistatic MIMO array framework (Jin et al., 2009; Chen et al., 2010; Koupatsiaris and Karystinos, 2013; Tang et al., 2013; Chen et al., 2014; Li and Zhang, 2014). Angle estimation is important in a bistatic MIMO array, and many joint direction of departure (DOD) and direction of arrival (DOA) target estimation methods in a bistatic MIMO array have been investigated (Chen DF et al., 2008; Chen JL et al., 2008; Yan et al., 2008; Zhang and Xu, 2010; Jiang et al., 2015; Xu et al., 2017). By exploiting the invariance properties of both transmit and receive arrays, the estimation of signal parameters via the rotational invariance technique (ESPRIT) method was applied for the estimation of DODs and DOAs in a bistatic MIMO array (Chen DF et al., 2008). Unfortunately, it still needs additional pair matching between DODs and DOAs of targets. To avoid the additional pair-matching problem, another ESPRIT method was proposed by Chen JL et al. (2008) to obtain automatically paired DODs and DOAs for target estimation by employing the interrelationship between invariance properties of the transmit and receive arrays.

The two-dimensional Capon (2D Capon) method for a bistatic MIMO array was proposed by Yan et al. (2008) to estimate DODs and DOAs of the targets. Unfortunately, the 2D Capon method requires a 2D peak search, leading to the high computational complexity. A reduced-dimension Capon (RD Capon) method was proposed by Zhang and Xu (2010), using the property of the Kronecker product. The high computational complexity of the 2D peak search for 2D Capon is avoided, but this method separately estimates DODs and DOAs of the targets. Then an estimated DOD-DOA pair-matching method was required, which adds computational loads. To avoid the added computational loads, Zhang and Zhu (2013) improved the RD Capon method and showed the estimation performance of the improved RD Capon method. The 2D multiple signal classification (2D MUSIC) method was to estimate DODs and DOAs in MIMO arrays (Li et al., 2005). The 2D MUSIC method shows excellent joint DOD and DOA estimation performance, but it is similar to the 2D Capon method because of its requirement for 2D angle peak searching renders which create high computational complexity. Using the same RD Capon theory, a reduced MUSIC

method (RD MUSIC) was proposed by Zhang and Xu (2010), which not only avoids the high computational complexity of the 2D MUSIC method, but also provides an excellent angle estimation performance. Bencheikh et al. (2010) proposed a polynomial root MUSIC method to estimate transmit and receive angles of targets with automatic pairing and to avoid the peak searching required in the MIMO 2D MUSIC method. Bencheikh and Wang (2010) proposed an algorithm combining the ESPRIT method with the root MUSIC approach to estimate the DODs and DOAs of targets without being paired in bistatic MIMO arrays.

In this study, the 2D MUSIC method in bistatic MIMO arrays is reviewed. An improved MUSIC estimator is proposed based on the Taylor expansion multiple signal classification (TE MUSIC) method. This estimator avoids the high computational complexity of 2D MUSIC and achieves automatically paired estimates of DODs and DOAs using two one-dimensional (1D) searches.

Notations:  $(\cdot)^T$  and  $(\cdot)^H$  denote transpose and conjugate transpose, respectively;  $\otimes$  stands for the Kronecker product;  $M_r M_t$  is the product of  $M_r$  and  $M_t$ ;  $\mathbf{I}_{M_r M_t}$  is an  $M_r M_t \times M_r M_t$  identity matrix;  $E(\cdot)$  stands for the expectation operation.

## 2 Signal model

Consider a narrowband bistatic MIMO array system with  $M_t$ -element transmit antennas and  $M_r$ -element receive antennas (Fig. 1). Both of the transmit and receive antennas are closely spaced in uniform linear arrays (ULAs). Elements of the arrays are omnidirectional, and the inter-element spaces in transmit and receive antennas are  $d_t$  and  $d_r$ , respectively. At the transmit site, transmit antennas simultaneously emit  $M$  different narrowband waveforms, which have the identical bandwidth and center frequency but are temporally orthogonal. Assume that the effect of Doppler frequency on the orthogonality of the waveforms can be ignored. There are  $P$  targets, which are located at  $(\theta_p, \phi_p)$  ( $p = 1, 2, \dots, P$ ) in the far field of the receive and transmit antennas, and all targets are assumed to locate at the same range bin from these antennas. Here,  $\phi_p$  is the DOD of the  $p^{\text{th}}$  target with respect to the transmit antennas, and  $\theta_p$  is the DOA of the  $p^{\text{th}}$  target with respect to the receive antennas. At the receive site,

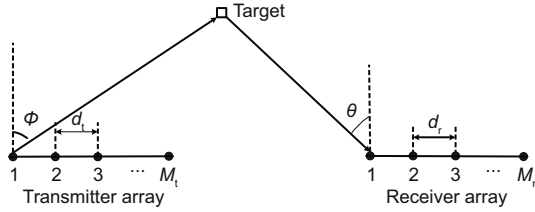


Fig. 1 Bistatic MIMO array framework

all antennas receive echoes from the targets for all transmitted waveforms. Thus, the outputs of the matched filters in all receivers can be expressed as (Xu et al., 2008)

$$\mathbf{y}(t) = \mathbf{A}\mathbf{s}(t) + \mathbf{n}(t), \quad (1)$$

where  $\mathbf{s}(t) = [s_1(t), s_2(t), \dots, s_P(t)]^T \in \mathbb{C}^{P \times 1}$  consists the amplitudes and phases of the  $P$  targets at time  $t$ .  $s_p(t) = \eta_p e^{j2\pi f_p t}$ , where  $\eta_p$  is the reflection coefficient and  $f_p$  the Doppler frequency.  $\mathbf{A}$  is an  $M_r M_t \times P$  matrix composed of the  $P$  steering vectors, expressed as

$$\mathbf{A} = [\mathbf{a}(\theta_1, \phi_1), \mathbf{a}(\theta_2, \phi_2), \dots, \mathbf{a}(\theta_P, \phi_P)], \quad (2)$$

where

$$\mathbf{a}(\theta_p, \phi_p) = \mathbf{a}_r(\theta_p) \otimes \mathbf{a}_t(\phi_p) \quad (3)$$

is the Kronecker product of the receive and transmit steering vectors for the  $p^{\text{th}}$  target, and

$$\mathbf{a}_r(\theta_p) = \left[ 1, e^{\frac{j2\pi d_r \sin \theta_p}{\lambda}}, \dots, e^{\frac{j2\pi (M_r - 1) d_r \sin \theta_p}{\lambda}} \right]^T, \quad (4)$$

$$\mathbf{a}_t(\phi_p) = \left[ 1, e^{\frac{j2\pi d_t \sin \phi_p}{\lambda}}, \dots, e^{\frac{j2\pi (M_t - 1) d_t \sin \phi_p}{\lambda}} \right]^T, \quad (5)$$

where  $\lambda$  is the wavelength. Here,  $\mathbf{a}_r(\theta_p)$  and  $\mathbf{a}_t(\phi_p)$  are the receive and transmit steering vectors for the  $p^{\text{th}}$  target, respectively.  $\mathbf{n}(t)$  is an  $M_r M_t \times 1$  complex Gaussian white noise vector with zero mean and covariance matrix of  $\sigma^2 \mathbf{I}_{M_r M_t}$ .

### 3 Taylor expansion multiple signal classification (TE MUSIC) estimator

In this section, a 2D MUSIC method is reviewed and a TE MUSIC method is derived.

#### 3.1 2D MUSIC method

The covariance matrix,  $\hat{\mathbf{R}}$ , can be achieved by

$$\hat{\mathbf{R}} = \frac{1}{I} \sum_{i=1}^I \mathbf{y}(t_i) \mathbf{y}^H(t_i), \quad (6)$$

where  $I$  is the snapshots. Using eigenvalue decomposition, the covariance matrix can be rewritten as

$$\hat{\mathbf{R}} = \mathbf{U}_S \mathbf{\Lambda}_S \mathbf{U}_S^H + \mathbf{U}_N \mathbf{\Lambda}_N \mathbf{U}_N^H, \quad (7)$$

where  $\mathbf{\Lambda}_S$  is a  $P \times P$  diagonal matrix, whose diagonal elements are the largest  $P$  eigenvalues. The other  $(M_r M_t - P)$  eigenvalues are the diagonal elements for the diagonal matrix  $\mathbf{\Lambda}_N$ .  $\mathbf{U}_S$  is a matrix composed of the eigenvectors of  $\hat{\mathbf{R}}$  arranged in descending order of the corresponding largest  $P$  eigenvalues.  $\mathbf{U}_N$  stands for the matrix containing other eigenvectors of  $\hat{\mathbf{R}}$ .  $\mathbf{U}_S$  and  $\mathbf{U}_N$  are the signal subspace and noise subspace, respectively. Furthermore,  $\mathbf{U}_S$  and  $\mathbf{U}_N$  are orthogonal. Then we have the following orthogonality condition:

$$\mathbf{a}^H(\theta, \phi) \mathbf{U}_N = \mathbf{0}. \quad (8)$$

The 2D MUSIC spectrum function can be constructed by

$$\mathbf{F}_{2D \text{ MUSIC}}(\theta, \phi) = \frac{1}{\mathbf{a}^H(\theta, \phi) \mathbf{U}_N \mathbf{U}_N^H \mathbf{a}(\theta, \phi)}. \quad (9)$$

Estimates of DOAs and DODs of targets can be achieved by searching the  $P$  largest peaks of  $\mathbf{F}_{2D \text{ MUSIC}}(\theta, \phi)$ . The estimation performance of the 2D MUSIC method is excellent. However, the method is inefficient due to the exhaustive 2D search. In the following subsections, the TE MUSIC method is presented to estimate DODs and DOAs of targets through two 1D searches to avoid the high computational complexity of the 2D MUSIC method.

#### 3.2 TE MUSIC method

The steering vector  $\mathbf{a}(\theta, \phi)$  can be approximated by a factorization. By exploiting an  $L$ -order Taylor expansion with respect to variable  $\phi$  at  $\phi = \phi_0$ , the factorization can be expressed as

$$\begin{aligned} \mathbf{a}(\theta, \phi) &\simeq \mathbf{a}(\theta, \phi_0) + \sum_{l=1}^L \mathbf{a}^{(l)}(\theta, \phi_0) \frac{(\phi - \phi_0)^l}{l!} \\ &= \mathbf{\Theta}(\theta) \mathbf{V}(\phi), \end{aligned} \quad (10)$$

where

$$\mathbf{\Theta}(\theta) = [\mathbf{a}(\theta, \phi_0), \mathbf{a}^{(1)}(\theta, \phi_0), \dots, \mathbf{a}^{(L)}(\theta, \phi_0)], \quad (11)$$

$$\mathbf{V}(\phi) = \left[ 1, (\phi - \phi_0), \dots, \frac{(\phi - \phi_0)^L}{L!} \right]^T, \quad (12)$$

and  $\mathbf{a}^{(l)}(\theta, \phi_0)$  is the  $l^{\text{th}}$  derivative of  $\mathbf{a}(\theta, \phi)$  evaluated at  $\phi = \phi_0$ .

Inserting Eq. (10) into Eq. (9), we obtain the TE MUSIC spectrum function as

$$\mathbf{F}_{\text{TE MUSIC}}(\theta, \phi) = \frac{1}{(\boldsymbol{\Theta}(\theta)\mathbf{V}(\phi))^{\text{H}} \mathbf{U}_N \mathbf{U}_N^{\text{H}} (\boldsymbol{\Theta}(\theta)\mathbf{V}(\phi))}. \quad (13)$$

Define

$$\mathbf{J}(\theta, \phi) = (\boldsymbol{\Theta}(\theta)\mathbf{V}(\phi))^{\text{H}} \mathbf{U}_N \mathbf{U}_N^{\text{H}} (\boldsymbol{\Theta}(\theta)\mathbf{V}(\phi)), \quad (14)$$

where

$$\begin{aligned} \mathbf{J}(\theta, \phi) &= (\boldsymbol{\Theta}(\theta)\mathbf{V}(\phi))^{\text{H}} \mathbf{U}_N \mathbf{U}_N^{\text{H}} (\boldsymbol{\Theta}(\theta)\mathbf{V}(\phi)) \\ &= \mathbf{V}^{\text{H}}(\phi) \boldsymbol{\Theta}^{\text{H}}(\theta) \mathbf{U}_N \mathbf{U}_N^{\text{H}} \boldsymbol{\Theta}(\theta) \mathbf{V}(\phi) \\ &= \mathbf{V}^{\text{H}}(\phi) \mathbf{Q}(\theta) \mathbf{V}(\phi) \end{aligned} \quad (15)$$

and

$$\mathbf{Q}(\theta) = \boldsymbol{\Theta}^{\text{H}}(\theta) \mathbf{U}_N \mathbf{U}_N^{\text{H}} \boldsymbol{\Theta}(\theta). \quad (16)$$

The TE MUSIC spectrum function can be rewritten as

$$\mathbf{F}_{\text{TE MUSIC}}(\theta, \phi) = \frac{1}{\mathbf{V}^{\text{H}}(\phi) \mathbf{Q}(\theta) \mathbf{V}(\phi)}. \quad (17)$$

Defining  $\mathbf{e} = [1, 0, \dots, 0]^{\text{T}} \in \mathbb{R}^{L \times 1}$ , we will obtain

$$\mathbf{e}^{\text{H}} \mathbf{V}(\phi) = 1. \quad (18)$$

Then the optimization problem of Eq. (17) can be reconstructed as

$$\min_{\theta, \phi} \mathbf{V}^{\text{H}}(\phi) \mathbf{Q}(\theta) \mathbf{V}(\phi) \text{ s.t. } \mathbf{e}^{\text{H}} \mathbf{V}(\phi) = 1. \quad (19)$$

Exploiting the Lagrange multiplier, the following cost function will be achieved first:

$$\mathbf{F}(\theta, \phi) = \mathbf{V}^{\text{H}}(\phi) \mathbf{Q}(\theta) \mathbf{V}(\phi) - \lambda_{\text{LM}} (\mathbf{e}^{\text{H}} \mathbf{V}(\phi) - 1), \quad (20)$$

where  $\lambda_{\text{LM}}$  is a constant. Then we have

$$\frac{\partial \mathbf{F}(\theta, \phi)}{\partial \mathbf{V}(\phi)} = 2\mathbf{Q}(\theta)\mathbf{V}(\phi) + \lambda_{\text{LM}}\mathbf{e} = 0. \quad (21)$$

With Eq. (21),  $\mathbf{V}(\phi)$  is

$$\mathbf{V}(\phi) = -\frac{\lambda_{\text{LM}}}{2} \mathbf{Q}^{-1}(\theta) \mathbf{e} = \beta \mathbf{Q}^{-1}(\theta) \mathbf{e}, \quad (22)$$

where  $\beta = -\lambda_{\text{LM}}/2$  and  $\beta$  is a constant. Combining Eqs. (18) and (22), we can obtain

$$\mathbf{e}^{\text{H}} \mathbf{V}(\phi) = \mathbf{e}^{\text{H}} \beta \mathbf{Q}^{-1}(\theta) \mathbf{e} = 1. \quad (23)$$

From Eq. (23),  $\beta$  can be given by

$$\beta = \frac{1}{\mathbf{e}^{\text{H}} \mathbf{Q}^{-1}(\theta) \mathbf{e}}. \quad (24)$$

Substituting Eq. (24) into Eq. (22),  $\mathbf{V}(\phi)$  is obtained by

$$\mathbf{V}(\phi) = \frac{\mathbf{Q}^{-1}(\theta) \mathbf{e}}{\mathbf{e}^{\text{H}} \mathbf{Q}^{-1}(\theta) \mathbf{e}}. \quad (25)$$

Then inserting  $\mathbf{V}(\phi)$  of Eq. (25) into the optimization problem (19), we achieve the estimates of DOAs via

$$\begin{aligned} \hat{\theta} &= \arg \min_{\theta} \frac{1}{\mathbf{e}^{\text{H}} \mathbf{Q}^{-1}(\theta) \mathbf{e}} \\ &= \arg \max_{\theta} \mathbf{e}^{\text{H}} \mathbf{Q}^{-1}(\theta) \mathbf{e}. \end{aligned} \quad (26)$$

The  $P$  largest peaks of the (1, 1) element of  $\mathbf{Q}^{-1}(\theta)$  will be achieved by searching  $\theta \in [-90^\circ, 90^\circ]$ . All these  $P$  largest peaks ( $\hat{\theta}_1, \hat{\theta}_2, \dots, \hat{\theta}_P$ ) correspond to the DOAs of targets. The DOD estimates can be easily obtained by substituting the DOAs into the 2D MUSIC spectrum function of Eq. (9) followed by another 1D search.

Because the  $p^{\text{th}}$  DOD is derived from the  $p^{\text{th}}$  DOA, the pairing between DOAs and DODs of the targets is automatically obtained, thus avoiding an additional pairing procedure.

Assume that  $N_{\text{T}}$  is the search time within one search range. Then the TE MUSIC method requires  $O((P+1) \times N_{\text{T}})$  search time, whereas the 2D MUSIC method needs  $O(N_{\text{T}}^2)$  search time. Therefore, the TE MUSIC method has a lower computational complexity than the 2D MUSIC method.

### 3.3 Steps of the TE MUSIC method

Steps of the TE MUSIC method are given as follows:

Step 1: Compute  $\hat{\mathbf{R}}$ , the covariance matrix of  $\mathbf{y}(t)$ .

Step 2: Obtain  $\boldsymbol{\Theta}(\theta)$  using an  $L$ -order Taylor expansion of  $\mathbf{a}(\theta, \phi)$  with respect to variable  $\phi$  at  $\phi = \phi_0$ .

Step 3: Calculate  $\mathbf{Q}(\theta) = \boldsymbol{\Theta}^{\text{H}}(\theta) \hat{\mathbf{R}}^{-1} \boldsymbol{\Theta}(\theta)$ .

Step 4: By searching  $\phi$ , we obtain the  $P$  largest peaks of the (1, 1) element of  $\mathbf{Q}^{-1}(\theta)$  to obtain the estimates of DOAs.

Step 5: Substitute the DOAs into the spectrum function and do another 1D search, and then we obtain the estimates of DODs.

## 4 Simulations and discussion

To verify the DOD and DOA estimation performances of the TE MUSIC method, Monte-Carlo tests are presented in this section.

Define the root mean squared error (RMSE) as

$$\text{RMSE} = \frac{1}{P} \sum_{p=1}^P \sqrt{\left(\psi_p - E(\hat{\psi}_p)\right)^2 + E\left(\left(\hat{\psi}_p - E(\hat{\psi}_p)\right)^2\right)}, \quad (27)$$

where  $\hat{\psi}_p$  is the estimate of the  $p^{\text{th}}$  target DOD/DOA.

Consider a bistatic MIMO array system with  $M_t = 8$  and  $M_r = 6$ , and assume that there are four uncorrelated targets located at angles of  $[\theta_1, \phi_1] = [10^\circ, 15^\circ]$ ,  $[\theta_2, \phi_2] = [40^\circ, 25^\circ]$ ,  $[\theta_3, \phi_3] = [20^\circ, 35^\circ]$ , and  $[\theta_4, \phi_4] = [30^\circ, 45^\circ]$ , respectively. Antennas of the arrays are spaced half a wavelength apart and the number of the snapshots is 200.  $\phi_0 = 30^\circ$  is for the fifth-order Taylor expansion.

Fig. 2 shows the paired results of the TE MUSIC method for four targets over 200 Monte-Carlo tests with signal-to-noise ratio (SNR) = 0 dB, and shows that the DODs and DOAs are correctly paired. The DODs and DOAs can be clearly observed.

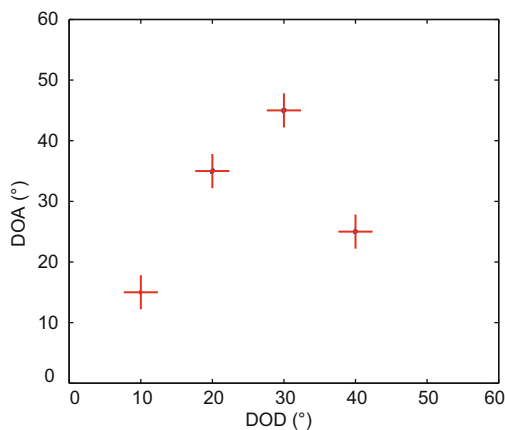


Fig. 2 Paired results of the TE MUSIC method for four targets from 200 Monte-Carlo tests with 0-dB SNR (crosses denote the real locations of the targets)

Figs. 3 and 4 present the comparisons of the DOA and DOD estimation performances with the 2D MUSIC method (Li et al., 2005), the RD MUSIC method (Zhang and Xu, 2010), and the ESPRIT method (Chen JL et al., 2008). Two hundred Monte-Carlo tests were used to achieve the RMSEs of these

four methods. As shown in Fig. 3, the DOA estimation RMSE of the ESPRIT method is the worst among these four methods. It is obvious that the TE MUSIC method has almost the same DOA estimation as the RD MUSIC method (Zhang and Xu, 2010). Due to the Taylor expansion of the steering vector, the DOA estimation performances of the TE MUSIC method and the RD MUSIC method are slightly worse than that of the 2D MUSIC method. In Fig. 4, the ESPRIT method has the worst DOD estimation RMSE among these four methods; the DOD estimation RMSEs of the TE MUSIC method and RD MUSIC method are similar to that of the 2D MUSIC method. Furthermore, with high SNRs, the DOD estimation performance of the TE MUSIC method is better than that of RD MUSIC. As mentioned in Section 3.2, the TE MUSIC method needs only two 1D searches, while the 2D MUSIC method requires an exhaustive 2D search.

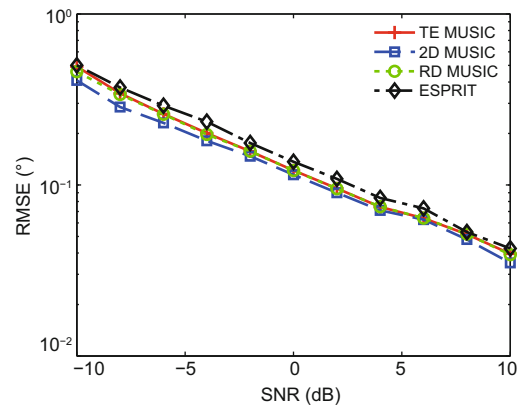


Fig. 3 RMSE of DOA estimation from 200 Monte-Carlo tests for four targets

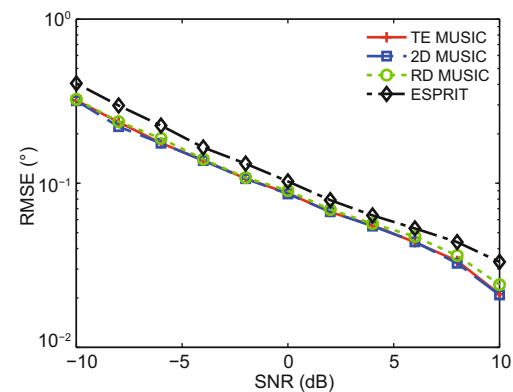


Fig. 4 RMSE of DOD estimation from 200 Monte-Carlo tests for four targets

Finally, the influence of  $\phi_0$  chosen by the TE MUSIC method is simulated in Figs. 5 and 6. The change range of  $\phi_0$  was  $[15^\circ, 20^\circ, 25^\circ, 30^\circ, 35^\circ, 40^\circ]$ . Two hundred Monte-Carlo tests were conducted to achieve the DOA and DOD estimation RMSEs for each SNR of each  $\phi_0$ . Figs. 5 and 6 show the DOD and DOA estimation performances of the TE MUSIC method with different  $\phi_0$ , respectively. It is clearly illustrated that the angle estimation performances of the TE MUSIC method with different  $\phi_0$  are similar, which means that the variety of  $\phi_0$  in  $[15^\circ, 20^\circ, 25^\circ, 30^\circ, 35^\circ, 40^\circ]$  has little effect on the angle estimation performance of the TE MUSIC method.

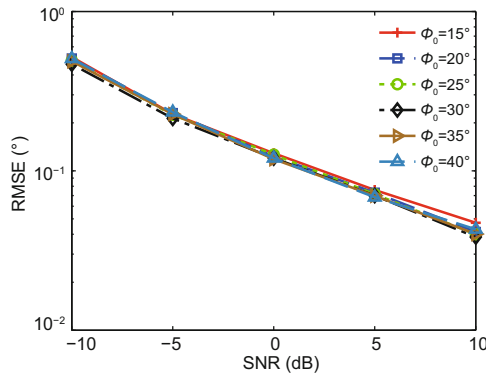


Fig. 5 RMSE of the DOA estimation from 200 Monte-Carlo tests with different  $\phi_0$  under the TE MUSIC method

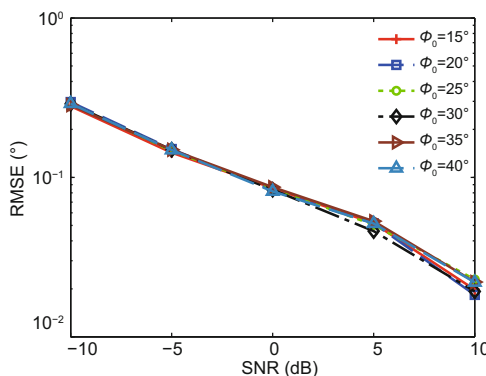


Fig. 6 RMSE of the DOD estimation from 200 Monte-Carlo tests with different  $\phi_0$  under the TE MUSIC method

## 5 Conclusions

In this paper, an improved MUSIC method has been presented that exploits the Taylor expansion of

the steering vector to avoid high computational cost of the 2D MUSIC method for DOD and DOA estimations in bistatic MIMO arrays. The TE MUSIC method could reduce the 2D search of the 2D MUSIC method to two 1D searches. Simulation results have verified that the TE MUSIC method has better DOD and DOA estimation performances compared with the ESPRIT method, and has performances that are very close to those of the 2D MUSIC and RD MUSIC methods. With high SNRs, the TE MUSIC method has a slightly better DOD estimation performance than the RD MUSIC method. Furthermore, the TE MUSIC method can automatically achieve paired DOD and DOA estimates.

## Compliance with ethics guidelines

Wen-tao SHI, Qun-fei ZHANG, Cheng-bing HE, and Jing HAN declare that they have no conflict of interest.

## References

- Ai Y, Yi W, Blum RS, et al., 2015. Cramer-Rao lower bound for multitarget localization with noncoherent statistical MIMO radar. *Proc IEEE Radar Conf*, p.1497-1502. <https://doi.org/10.1109/RADAR.2015.7131233>
- Bekkerman I, Tabrikian J, 2006. Target detection and localization using MIMO radars and sonars. *IEEE Trans Signal Proc*, 54(10):3873-3883. <https://doi.org/10.1109/TSP.2006.879267>
- Bencheikh ML, Wang Y, 2010. Joint DOD-DOA estimation using combined ESPRIT-MUSIC approach in MIMO radar. *Electron Lett*, 46(15):1081-1083. <https://doi.org/10.1049/el.2010.1195>
- Bencheikh ML, Wang Y, He HY, 2010. Polynomial root finding technique for joint DOA DOD estimation in bistatic MIMO radar. *Signal Proc*, 90(9):2723-2730. <https://doi.org/10.1016/j.sigpro.2010.03.023>
- Cao RZ, Liu BY, Gao FF, et al., 2017. A low-complex one-snapshot DOA estimation algorithm with massive ULA. *IEEE Commun Lett*, 21(5):1071-1074. <https://doi.org/10.1109/LCOMM.2017.2652442>
- Chen DF, Chen BX, Qian GD, 2008. Angle estimation using ESPRIT in MIMO radar. *Electron Lett*, 44(12):770-771. <https://doi.org/10.1049/el:20080276>
- Chen HW, Li X, Wang HQ, et al., 2014. Performance bounds of direction finding and its applications for multiple-input multiple-output radar. *IET Radar Sonar Nav*, 8(3):251-263. <https://doi.org/10.1049/iet-rsn.2013.0119>
- Chen JL, Gu H, Su WM, 2008. Angle estimation using ESPRIT without pairing in MIMO radar. *Electron Lett*, 44(24):1422-1423. <https://doi.org/10.1049/el:20089089>
- Chen JL, Gu H, Su WM, 2010. A new method for joint DOD and DOA estimation in bistatic MIMO radar. *Signal Proc*, 90(2):714-718. <https://doi.org/10.1016/j.sigpro.2009.08.003>

- Fishler E, Haimovich A, Blum R, et al., 2004a. MIMO radar: an idea whose time has come. *Proc IEEE Radar Conf*, p.71-78. <https://doi.org/10.1109/NRC.2004.1316398>
- Fishler E, Haimovich A, Blum R, et al., 2004b. Performance of MIMO radar systems: advantages of angular diversity. *Proc 38<sup>th</sup> Asilomar Conf on Signals, Systems and Computers*, p.305-309. <https://doi.org/10.1109/ACSSC.2004.1399142>
- Fishler E, Haimovich A, Blum R, et al., 2006. Spatial diversity in radars—models and detection performance. *IEEE Trans Signal Proc*, 54(3):823-838. <https://doi.org/10.1109/TSP.2005.862813>
- Guo YD, Feng CQ, Zhang YS, et al., 2015. Joint DOD and DOA estimation for bistatic MIMO radar with combined array errors. *Proc IET Int Radar Conf*, p.1-5. <https://doi.org/10.1049/cp.2015.1472>
- Haimovich AM, Blum RS, Cimini LJ, 2008. MIMO radar with widely separated antennas. *IEEE Signal Proc Mag*, 25(1):116-129. <https://doi.org/10.1109/MSP.2008.4408448>
- Jiang H, Zhang JK, Wong KM, 2015. Joint DOD and DOA estimation for bistatic MIMO radar in unknown correlated noise. *IEEE Trans Veh Technol*, 64(11):5113-5125. <https://doi.org/10.1109/TVT.2014.2384495>
- Jin M, Liao GS, Li J, 2009. Joint DOD and DOA estimation for bistatic MIMO radar. *Signal Proc*, 89(2):244-251. <https://doi.org/10.1016/j.sigpro.2008.08.003>
- Koupsiaris DA, Karystinos GN, 2013. Efficient DOA, DOD, and target estimation for bistatic MIMO sonar. *Proc IEEE Int Conf on Acoustics, Speech and Signal Processing*, p.5155-5159. <https://doi.org/10.1109/ICASSP.2013.6638645>
- Li J, Stoica P, 2007. MIMO radar with colocated antennas. *IEEE Signal Proc Mag*, 24(5):106-114. <https://doi.org/10.1109/MSP.2007.904812>
- Li J, Conan J, Pierre S, 2005. Joint estimation of channel parameter for MIMO communication systems. *Proc 2<sup>nd</sup> Int Symp on Wireless Communication Systems*, p.22-26. <https://doi.org/10.1109/ISWCS.2005.1547647>
- Li JF, Zhang XF, 2014. Unitary subspace-based method for angle estimation in bistatic MIMO radar. *Circ Syst Signal Proc*, 33(2):501-513. <https://doi.org/10.1007/s00034-013-9653-9>
- Robey FC, Coutts S, Weikle D, et al., 2004. MIMO radar theory and experimental results. *Proc 38<sup>th</sup> Asilomar Conf on Signals, Systems and Computers*, p.300-304. <https://doi.org/10.1109/ACSSC.2004.1399141>
- Sharify S, Nayebi MM, 2017. Approach to detector design for statistical multiple-input–multiple-output radars using multi-scan data. *IET Radar Sonar Nav*, 11(4):664-672. <https://doi.org/10.1049/iet-rsn.2016.0328>
- Tang B, Tang J, Zhang Y, et al., 2013. Maximum likelihood estimation of DOD and DOA for bistatic MIMO radar. *Signal Proc*, 93(5):1349-1357. <https://doi.org/10.1016/j.sigpro.2012.11.011>
- Xu BQ, Zhao YB, Cheng ZF, et al., 2017. A novel unitary PARAFAC method for DOD and DOA estimation in bistatic MIMO radar. *Signal Proc*, 138:273-279. <https://doi.org/10.1016/j.sigpro.2017.03.016>
- Xu LZ, Li J, Stoica P, 2008. Target detection and parameter estimation for MIMO radar systems. *IEEE Trans Aerosp Electron Syst*, 44(3):927-939. <https://doi.org/10.1109/TAES.2008.10299612>
- Yan HD, Liao GS, Li J, 2008. Multitarget identification and localization using bistatic MIMO radar systems. *EURASIP J Adv Signal Proc*, Article 283483. <https://doi.org/10.1155/2008/283483>
- Yeo K, Chung Y, Yang H, et al., 2017. Reduced-dimension DOD and DOA estimation through projection filtering in bistatic MIMO radar with jammer discrimination. *IET Radar Sonar Nav*, 11(8):1228-1234. <https://doi.org/10.1049/iet-rsn.2016.0627>
- Zhang SN, Zhu XH, 2013. Improved design of unimodular waveforms for MIMO radar. *Multidim Syst Signal Proc*, 24(3):447-456. <https://doi.org/10.1007/s11045-011-0171-2>
- Zhang X, Xu D, 2010. Angle estimation in MIMO radar using reduced-dimension Capon. *Electron Lett*, 46(12):860-861. <https://doi.org/10.1049/el.2010.0346>
- Zheng GM, Chen BX, 2015. Unitary dual-resolution ESPRIT for joint DOD and DOA estimation in bistatic MIMO radar. *Multidim Syst Signal Proc*, 26(1):159-178. <https://doi.org/10.1007/s11045-013-0244-5>
- Zheng GM, Tang J, Yang X, 2016. ESPRIT and unitary ESPRIT algorithms for coexistence of circular and non-circular signals in bistatic MIMO radar. *IEEE Access*, 4:7232-7240. <https://doi.org/10.1109/ACCESS.2016.2624561>